# Electronic Supplementary Information

# Fabricating defect-rich metal-organic frameworks via mixed-linker induced crystal transformation

Yue Xiao,[a] Lu Han,[a] Jihai Tang,[a] Lifang Tian,[b] Zhuxiu Zhang,*[a] Lixiong Zhang,*[a] Dong Yang*[a] and Xu Qiao[a]

[a]State Key Laboratory of Materials-Oriented Chemical Engineering, College of Chemical Engineering, Nanjing Tech University, Nanjing 211816, China.
[b]Institute of Advanced Synthesis (IAS), School of Chemistry and Molecular Engineering, Nanjing Tech University, Nanjing 211816, China.

*E-mail: zhuxiu.zhang@njtech.edu.cn (Zhuxiu Zhang); lixiongzhang@njtech.edu.cn (Lixiong Zhang); dyang@njtech.edu.cn (Dong Yang)

# EXPERIMENTAL SCETION

## Chemicals

$ZrCl_4$ (99.0%), N,N-dimethylformamide (DMF; 99.5%) and KBr (99.0%) were obtained from Sinopharm. 2-nitro-1,4-benzenedicarboxylicacid ($H_2BDC\text{-}NO_2$; 98%), 2-amino-1,4-benzenedicarboxylicacid ($H_2BDC\text{-}NH_2$; 98%) and benzene-1,4-dicarboxylic acid ($H_2BDC$; 99%), was obtained from Macklin. Acetic acid (AA; 99%) was obtained from Aladdin. Acetone was obtained from Lingfeng Chemical Reagent (99.5%). $D_2O$ (99.9%) was obtained from Nanjing Haolv Biotech. NaOH (96.0%) was obtained from Xilong Scientific. All commercial chemicals and reagents were used as received without further purification.

## Materials synthesis

**Synthesis of mixed-linker UiO-66.** $ZrCl_4$ (0.8 g, 3.43 mmol) and modulator (acetic acid, 5.89 mL) was dissolved in 133.33 mL of DMF in a 200-mL Teflon liner under sonication. The linker precursor, $H_2BDC\text{-}NO_2$ (0, 0.68, 1.37, 2.01, 2.74 and 3.43 mmol) and $H_2BDC\text{-}NH_2$ (3.43, 2.74, 2.01, 1.37, 0.68 and 0 mmol), were then added to the solution and dissolved by ultrasound for 15 min at room temperature. The Teflon liner was then sealed in an autoclave and heated in a 120 ℃ oven for 24 h. After cooling to room temperature, the mother liquor was decanted and the precipitates were isolated by centrifugation. The solids were washed with DMF (30 mL) three times in a day to remove unreacted precursors and with acetone (30 mL) six times in 2 days to remove DMF. Then, the powder was dried at room temperature and activated at 120 ℃ under dynamic vacuum for 12 h prior to characterization.

**Mixed-linker induced crystal transformation from fcu to hcp.** Mixed-linker UiO-66 (150 mg), $H_2O$ (10 mL) and acetic acid (10 mL) were mixed in a 50-mL Teflon liner under sonication. The Teflon liner was then sealed in an autoclave and heated in a 150 ℃ oven for 24 h. After cooling to room temperature, the upper liquid was decanted and the solids were isolated by centrifugation. The solids were washed with DMF for three times and further washed with acetone for six times. Then, the powder was dried at room temperature and activated at 120 ℃ under dynamic vacuum for 12 h prior to characterization and catalysis.

**Synthesis of UiO-66.** $ZrCl_4$ (0.8 g, 3.43 mmol) and modulator (acetic acid, 5.89 mL) was dissolved in 133.33 mL of DMF in a 200-mL Teflon liner under sonication. The linker precursor ($H_2BDC$, 0.57 g, 3.43 mmol) was then added to the solution and dissolved by ultrasound for 15 min at room temperature. The Teflon liner was then sealed in an autoclave and heated in a 120 ℃ oven for 24 h. After cooling to room temperature, the mother liquor was decanted and the precipitates were isolated by centrifugation. The solids were washed with DMF (30 mL) three times in a day to remove unreacted precursors and with acetone (30 mL) six times in 2 days to remove DMF. Then, the powder was dried at room temperature and activated at 120 ℃ under dynamic vacuum for 12 h prior to characterization.

**Synthesis of hcp UiO-66.** $ZrOCl_2 \cdot 8H_2O$ (0.242 g, 0.75 mmol) was dissolved in 5 mL of $H_2O$ in a 50-mL Teflon liner under sonication. The linker precursor ($H_2BDC$, 0.093 g, 0.56 mmol) and modulator (acetic acid, 7.5 mL) were then added to the solution, which was further sonicated for ~15 min at room temperature. The Teflon liner was then sealed in an autoclave and heated in a 150 ℃ oven for 24 h. After cooling to room temperature, the mother liquor was decanted and the precipitates were isolated by centrifugation. The solids were washed with DMF (30 mL) three times in a day to remove unreacted precursors and with acetone (30 mL) six times in 2 days to remove DMF. Then, the powder was dried at room temperature and activated at 120 ℃ under dynamic vacuum for 12 h prior to characterization.

**Synthesis of hcp UiO-66.** $ZrOCl_2 \cdot 8H_2O$ (0.242 g, 0.75 mmol) was dissolved in 5 mL of $H_2O$ in a 50-mL Teflon liner under sonication. The linker precursor ($H_2BDC$, 0.093 g, 0.56 mmol) and modulator (acetic acid, 7.5 mL) were then added to the solution, which was further sonicated for ~15 min at room temperature. The Teflon liner was then sealed in an autoclave and heated in a 150 ℃ oven for 24 h. After cooling to room temperature, the mother liquor was decanted and the precipitates were isolated by centrifugation. The solids were washed with DMF (30 mL) three times in a day to remove unreacted precursors and with acetone (30 mL) six times in 2 days to remove DMF. Then, the powder was dried at room temperature and activated at 120 ℃ under dynamic vacuum for 12 h prior to characterization.

**Synthesis of hcp UiO-66-$NO_2$ with low defect concentration.** UiO-66-$NO_2$ (150 mg), $H_2O$ (8 mL) and formic acid (8 mL) were mixed in a 50-mL Teflon liner under sonication. The Teflon liner was then sealed in an autoclave and heated in a 150 ℃ oven for 24 h. After cooling to room temperature, the upper liquid was decanted and the solids were isolated by centrifugation. The solids were washed with DMF for three times and further washed with acetone for six times. Then, the powder was dried at room temperature and activated at 120 ℃ under dynamic vacuum for 12 h prior to characterization and catalysis. This sample was denoted as **hcp** $NO_2$-FA.

## Characterization

**Powder X-ray diffraction (PXRD).** PXRD patterns of all MOF samples were recorded using a Rigaku SmartLab 9 kW X-ray diffractometer in the 2θ range from 3° to 40° at 40 kV and 100 mA along with the scanning speed of 5°/min.

**$N_2$ sorption isotherms.** $N_2$ sorption isotherms were measured by a Micromeritics TriStar II surface area and porosity analyzer at 77 K. Prior to analysis, the sample was evacuated at 120 ℃ for 12 h. The Brunauer−Emmett−Teller (BET) surface area was calculated with the relative pressure ranging from 0.05 to 0.35 and the pore size distribution was analyzed by nonlocal density functional theory (NLDFT) model.

**Infrared spectroscopy.** Fourier transform infrared (FT-IR) spectra of the MOF samples were carried out on a Bruker VERTEX 70v vacuum FT-IR spectrometer with a spectra resolution of 2 $cm^{-1}$. Approximately 5.0 mg of the MOF sample was mixed with dry KBr powder and loaded in a Harrick DRIFTS cell in an $N_2$-filled glove box. The sample

cell was then transferred to the measurement chamber of the FT-IR spectrometer and the IR spectrum was recorded with the sample in flowing $N_2$ at certain temperature. Each spectrum was the average of 32 scans.

**MOF sample digestion and characterization by $^1$H NMR spectroscopy.** Typically, 10 mg activated MOF sample and 40 mg NaOH were mixed with 1 mL of $D_2O$ in a vial. The vial was capped and inverted 2-3 times before leaving the sample to digest over a period of 24 h. After 24 h, the supernatant was transferred into an NMR tube. The $^1$H NMR spectra were recorded with a Bruker Avance III 400 NMR spectrometer (400 MHz). The relaxation delay (d1) was set to 20 s to ensure that reliable integrals were obtained, allowing for the accurate determination of the relative concentrations of the molecular components. The number of scans per sample was 16.

**Thermal gravimetric Analysis (TGA).** Thermogravimetric analyses were performed on Mettler Toledo TGA/DSC at 10 °C/min$^{-1}$ under $O_2$ with a flow rate of 25 mL/min.

**Scanning electron microscopy (SEM).** SEM images of the MOF samples were collected on the FEI Quanta electron microscope at an accelerating voltage of 5.0 kV. Energy dispersive X-ray spectroscopy (EDS). was performed in the scanning electron (SE) mode, and the accelerating voltage was 20 kV.

**Inductively coupled plasma atomic-emission spectrometer (ICP-AES).** The dissolved $Zr^{4+}$ during crystal transformation was quantified by the Jarrell-Ash 1100 instrument.

**Elemental analysis (EA).** EA was performed on a Perkin Elmer 2400 Series II CHNS elemental analyzer to quantify carbon, hydrogen and nitrogen in samples.

## Catalytic test

Typically, styrene oxide (0.29 mmol), alcohol (24.7 mmol) and activated MOF catalyst (1 mol % of styrene oxide) were mixed in a 2.0 mL Pyrex vial. The sealed vial was than loaded in a thermo-shaker and the reaction was conducted at 55 ℃ for 2 h under a shake speed of 1000 rpm. After reaction, the supernatant was recovered by certification and analyzed by gas chromatograph (GC, FULI Analytical GC9790Plus) equipped with FID and a SE-54 column.

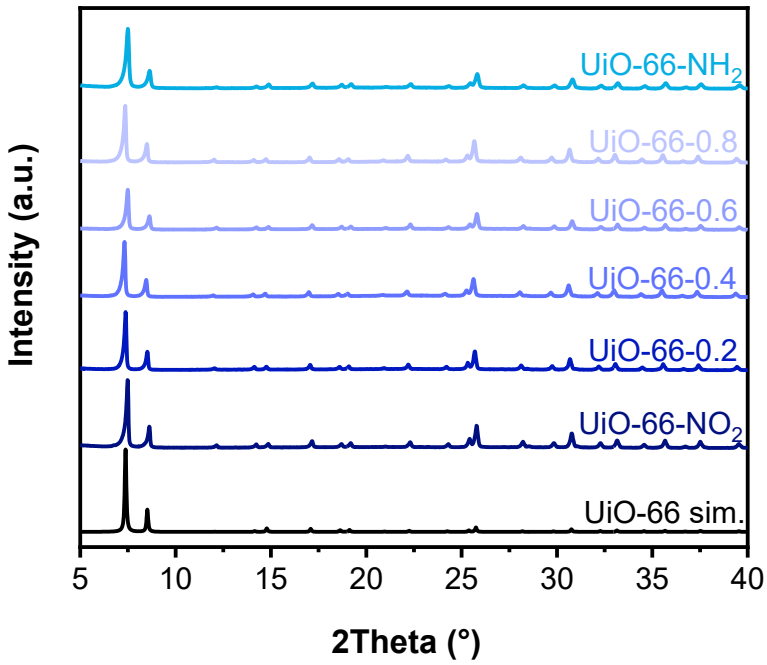


**Figure S1.** PXRD patterns of UiO-66-$NO_2$, UiO-66-$NH_2$ and the mixed-linker UiO-66 samples.

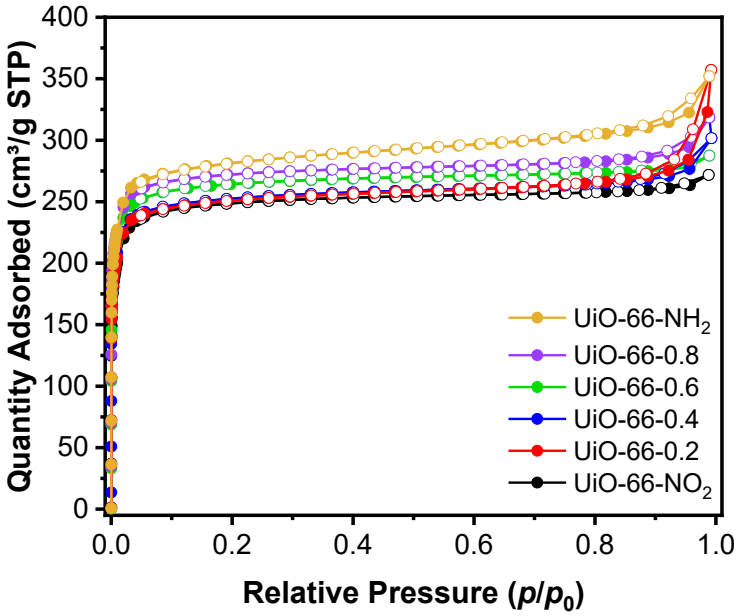


**Figure S2.** $N_2$ sorption isotherms of UiO-66-$NO_2$, UiO-66-$NH_2$ and the mixed-linker UiO-66 samples.

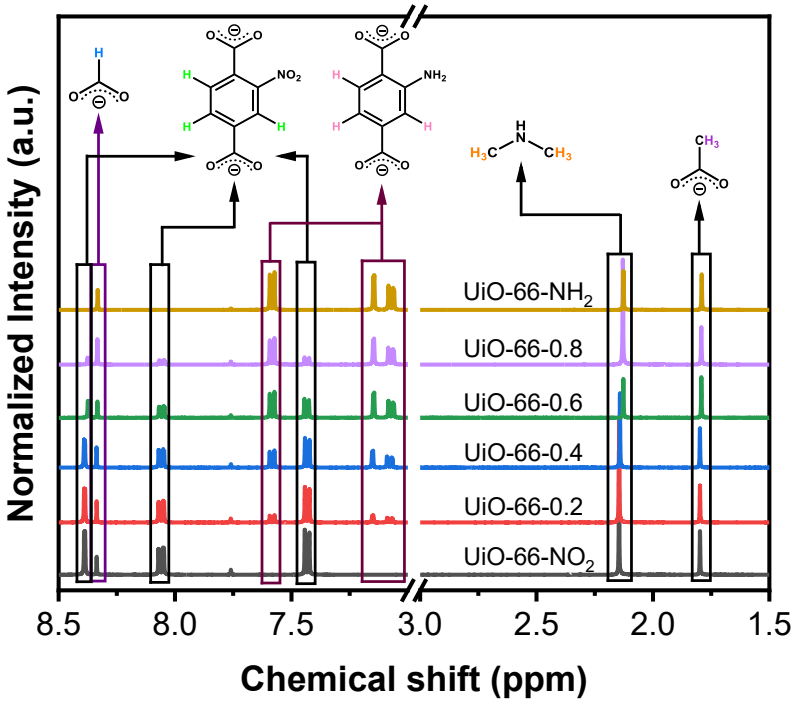


**Figure S3.** $^{1}$H NMR spectra of digested UiO-66-$NO_2$, UiO-66-$NH_2$ and the mixed-linker UiO-66 samples in NaOH/$D_2O$.

**Table S1.** BET surface areas, molar fraction of $NH_2$-BDC linker and the number of nonlinker ligands per node of the MOF samples.

| MOF sample | $S_{BET}$ ($m^2$/g) | Molar fraction of $NH_2$-BDC (%) | Number of ligands per node | |
|---|---|---|---|---|
| | | | formate | acetate |
| UiO-66-$NO_2$ | 889 | 0 | 0 | 0.88 |
| UiO-66-0.2 | 894 | 20.1 | 0 | 0.80 |
| UiO-66-0.4 | 896 | 36.6 | 0.10 | 0.77 |
| UiO-66-0.6 | 901 | 57.3 | 0.12 | 0.77 |
| UiO-66-0.8 | 970 | 76.7 | 0.32 | 0.95 |
| UiO-66-$NH_2$ | 1003 | 100 | 0.86 | 0.88 |
| UiO-66-H | 1137 | 0 | 0.28 | 0.91 |
| **hcp** UiO-66 | 632 | 0 | 0 | 0.96 |

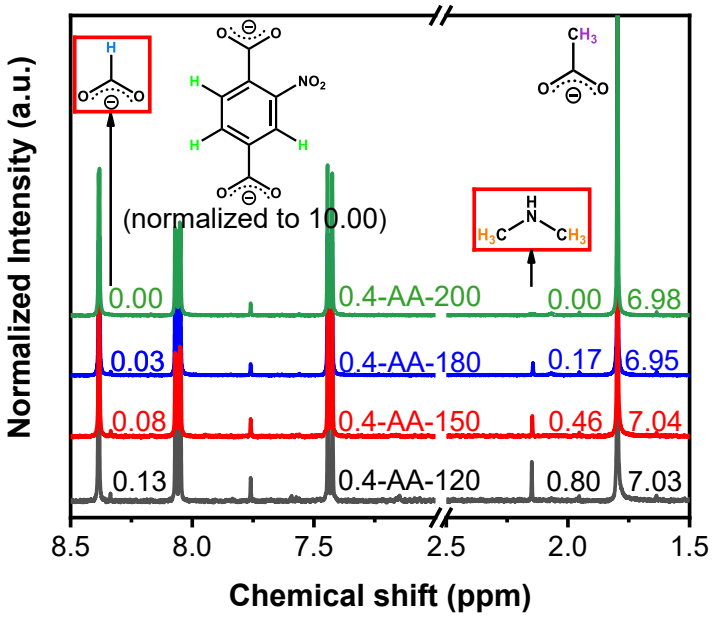


**Figure S4.** $^{1}$H NNMR spectra of digested 0.4-AA activated at 120, 150, 180 and 200 ℃.

Before $^{1}$H NMR test, the MOF sample was digested in NaOH/$D_2O$ solution. Only the organic portion (linker, modulator, DMF, etc.) can be dissolved in the solution and the inorganic components were filtered out. Especially, the residual DMF in MOFs will decompose into equimolar amounts formate and $HN(CH_3)_2$ in NaOH/$D_2O$ solution. Take 0.4-AA as an example, the molar ratio of $HN(CH_3)_2$:formate is 1:1 as shown in figure S4. According to our recent work,[1] the residual DMF in UiO-66 can be evacuated at temperatures above 200 ℃. Hence, we activated 0.4-AA at evaluated temperatures (150, 180 and 200 ℃) for 12 h and tested their digested $^{1}$H NMR spectra. As shown in Figure S4, formate and $HN(CH_3)_2$ decreased equally with the increasing temperature and were both totally removed after activation at 200 ℃. These results demonstrate that $HN(CH_3)_2$ and formate detected in $^{1}$H NMR spectra are both derived from the residual DMF rather than coordinated to defects. Besides, the peak area of acetate remained almost unchanged indicating that only acetate ligands are bonded to defect sites.

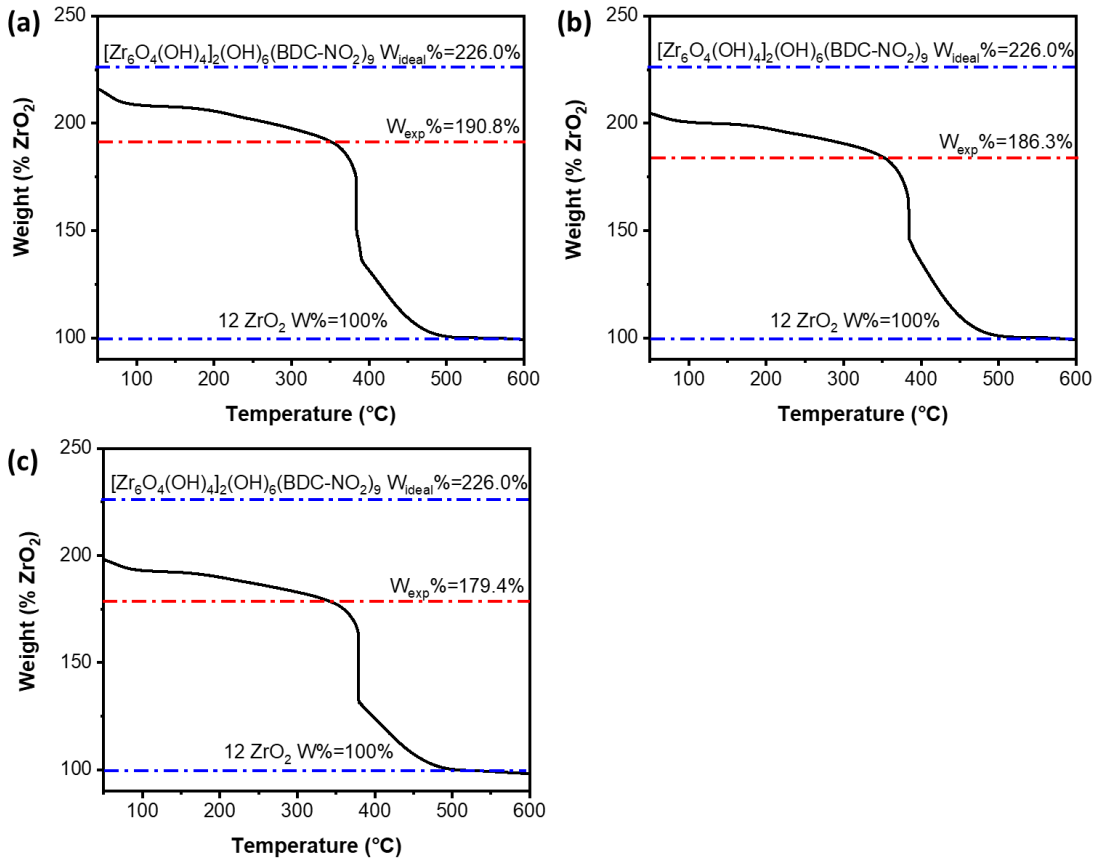


**Figure S5.** TGA curves measured in the flow of $O_2$ of 0.2-AA (a), 0.4-AA (b) and 0.6-AA (c).

**Table S2.** Numbers of defects in **hcp** UiO-66-$NO_2$ determined by TGA.

| Samples | Defects per MOF node |
|---|---|
| 0.2-AA | 4.3 |
| 0.4-AA | 4.9 |
| 0.6-AA | 5.9 |

**Table S3.** Molar ratio of C:N in **hcp** UiO-66-$NO_2$.

| Samples | C:N (mol/mol) | |
|---|---|---|
| | determined by $^1$H NMR | determined by EA |
| 0.2-AA | 9.2 | 9.7 |
| 0.4-AA | 9.4 | 10.1 |
| 0.6-AA | 9.7 | 10.5 |

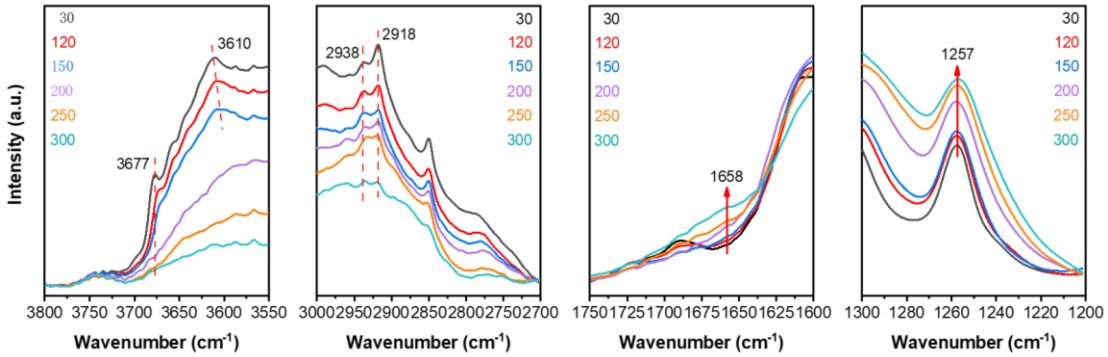


**Figure S6.** IR spectra of 0.4-AA in flowing $N_2$ as the temperature was ramped from 30 to 300 °C. Colored numbers represent temperatures in °C.

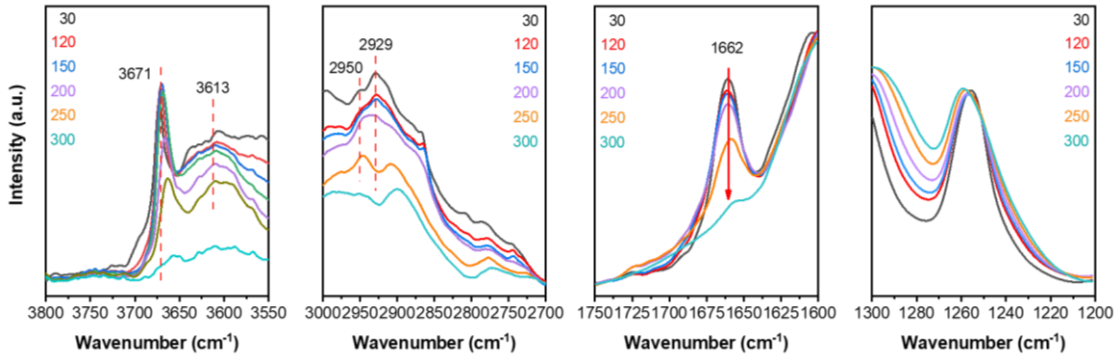


**Figure S7.** IR spectra of UiO-66-$NO_2$ in flowing $N_2$ as the temperature was ramped from 30 to 300 °C. Colored numbers represent temperatures in °C.

Variable-temperature infrared (IR) spectroscopy was carried out to determine the chemical composition and thermal stability of the UiO-66-$NO_2$ and **hcp** UiO-66-$NO_2$. 0.4-AA was selected as the proxy of defective **hcp** UiO-66-$NO_2$ owing to its high crystallinity and defect concentration. ν(OH) band of the $\mu_3$-OH groups on the $Zr_{12}O_{22}$ node is observed at 3677 $cm^{-1}$, which is consistent with that in the $Zr_6O_8$ based UiO-66-$NO_2$ (3671 $cm^{-1}$). A broad band centred at about 3610 $cm^{-1}$ is observed in both UiO-66-$NO_2$ and **hcp** UiO-66-$NO_2$ indicating the presence of a mass of H-bonded water molecules in these samples, and these water molecules cannot be completely removed even at 300 °C. The the band at 1662 $cm^{-1}$ in IR spectra of UiO-66-$NO_2$ is correlated to water bonded unidentate monocarboxylate groups on defect sites according to a recent study.[2] This band gradually diminished upon raising the temperature owing to the removal of H-bonded water.

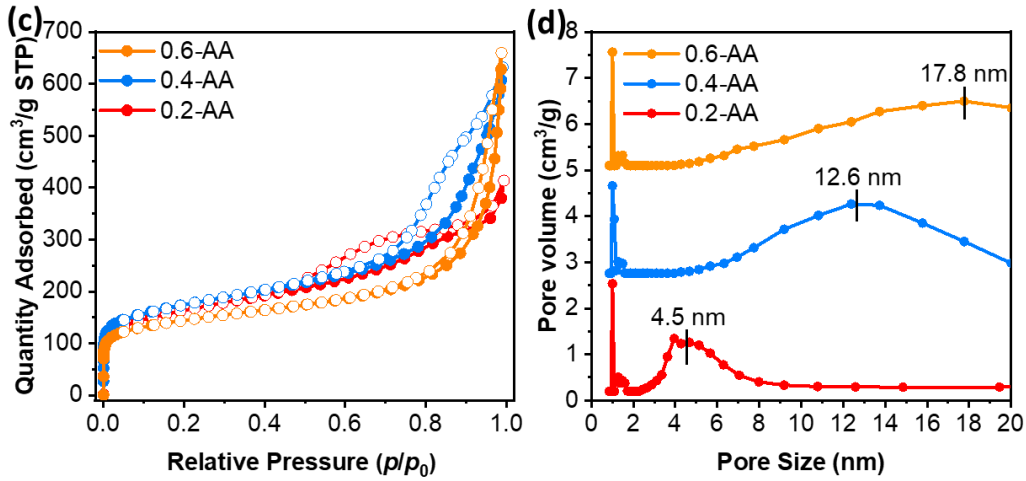


**Figure S8.** $N_2$ sorption isotherms (a) and NLDFT pore size distributions (b) of 0.2-AA, 0.4-AA and 0.6-AA.

**Table S4.** Numbers of acetate ligands per $Zr_{12}$ node determined by $^1H$ NMR spectroscopy and porosity parameters of the MOF samples prepared via MICT.

| Samples | Acetate ligands per node | $V_{micro}$ ($cm^3/g$) | $V_{meso}$ ($cm^3/g$) | $S_{BET}$ ($m^2/g$) |
|---|---|---|---|---|
| 0.2-AA | 4.08 | 0.35 | 0.54 | 585 |
| 0.4-AA | 4.68 | 0.27 | 0.83 | 624 |
| 0.6-AA | 5.33 | 0.11 | 0.90 | 473 |

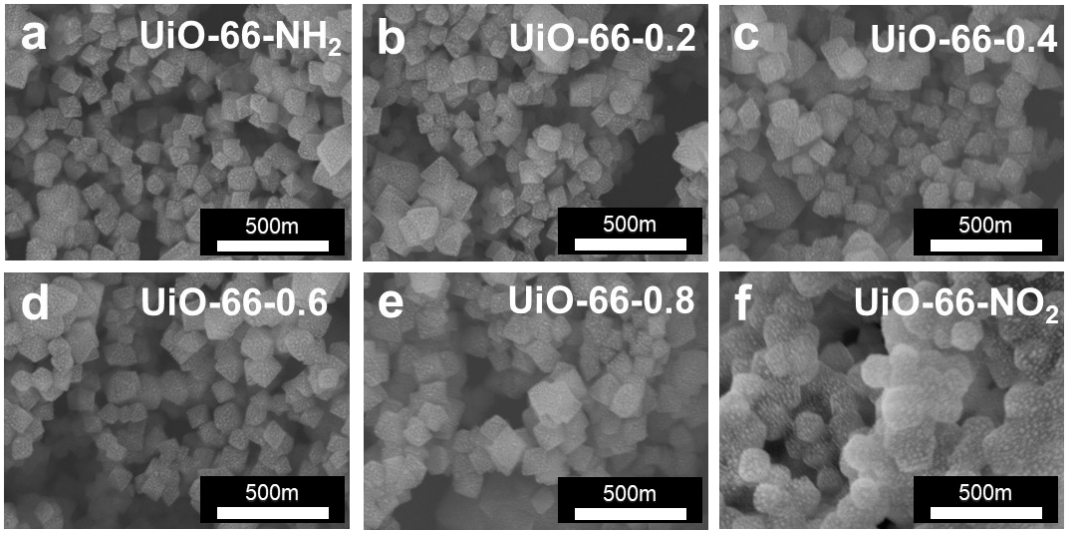


**Figure S9.** SEM images of UiO-66-$NO_2$, UiO-66-$NH_2$ and the mixed-linker UiO-66 samples.

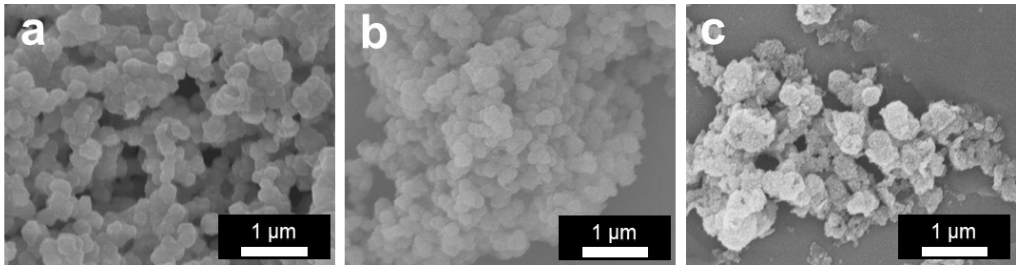


**Figure S10.** SEM images of 0.2-AA (a), 0.4-AA (b) and 0.6-AA (c).

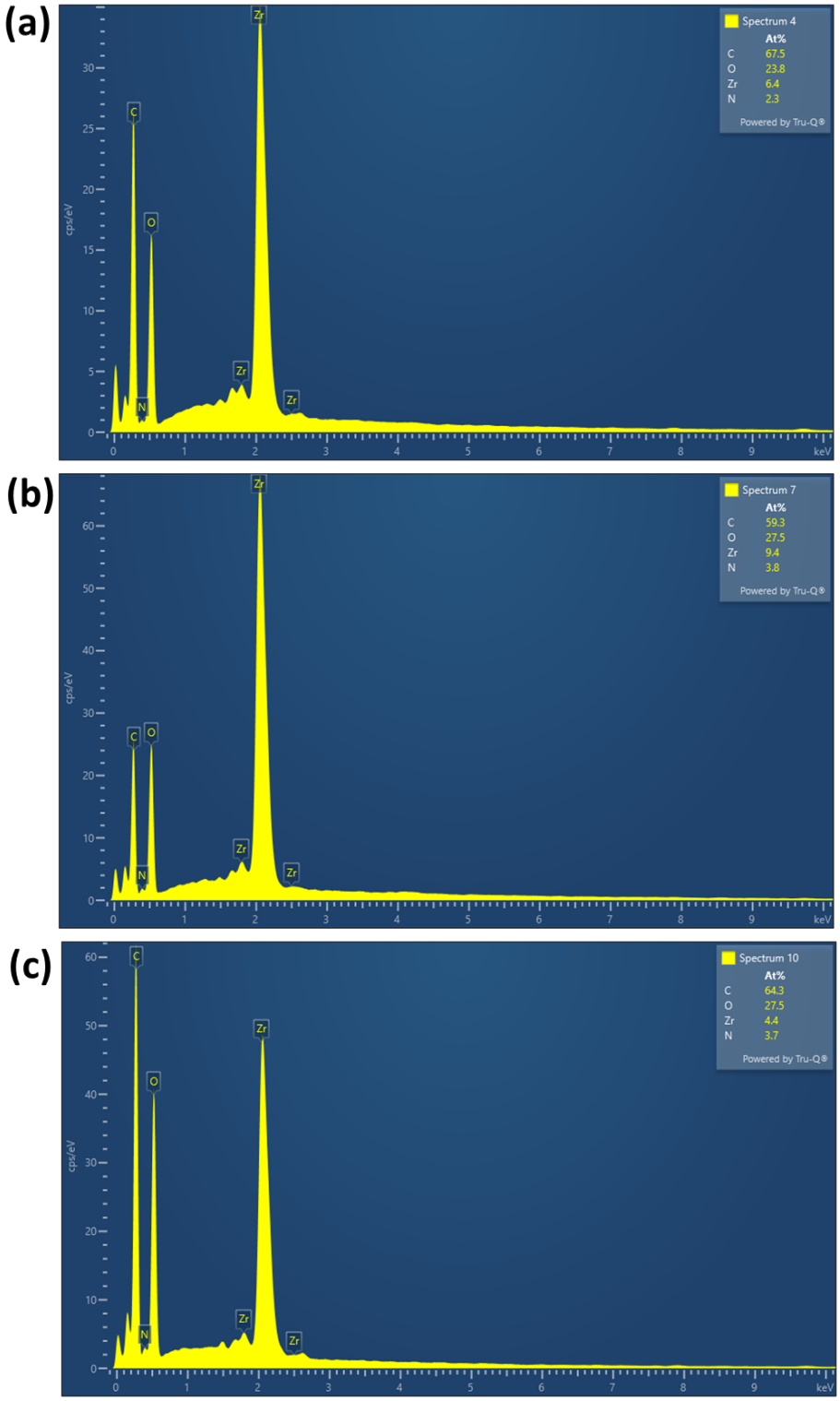


**Figure S11.** EDS analysis of 0.2-AA (a), 0.4-AA (b) and 0.6-AA (c).

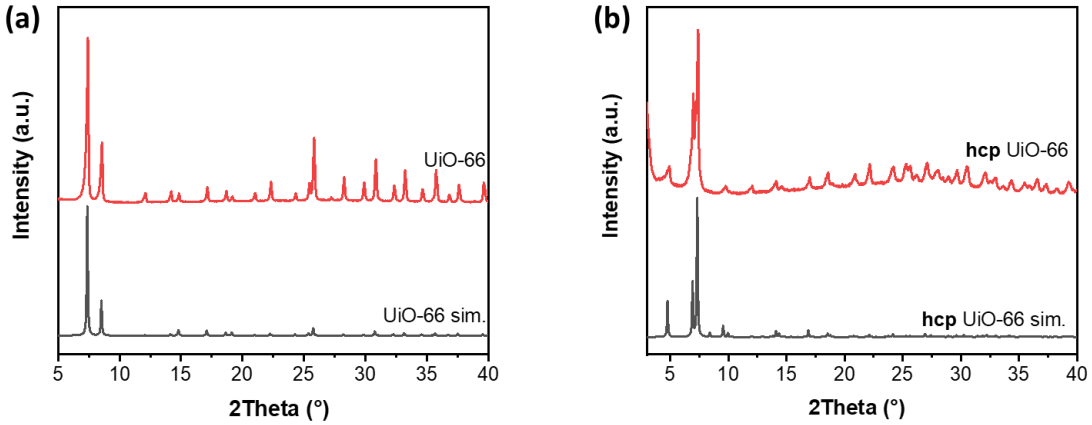


**Figure S12.** PXRD patterns of UiO-66 (a) and **hcp** UiO-66 (b).

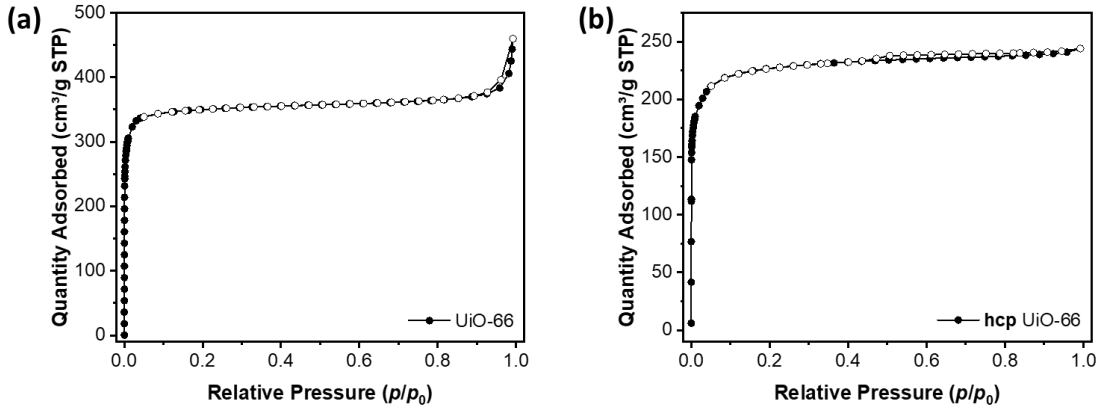


**Figure S13.** $N_2$ sorption isotherms of UiO-66 (a) and **hcp** UiO-66 (b).

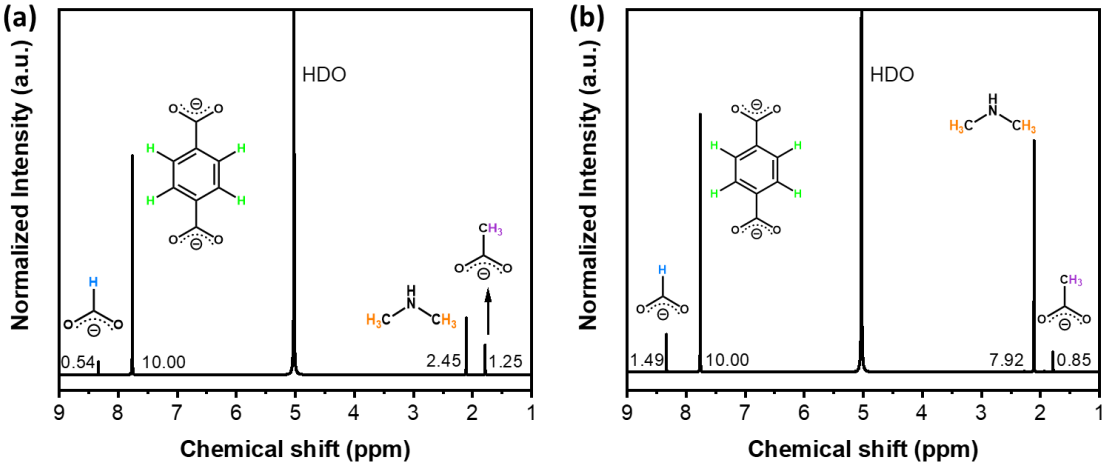


**Figure S14.** $^1$H NMR spectra of UiO-66 (a) and **hcp** UiO-66 (b).

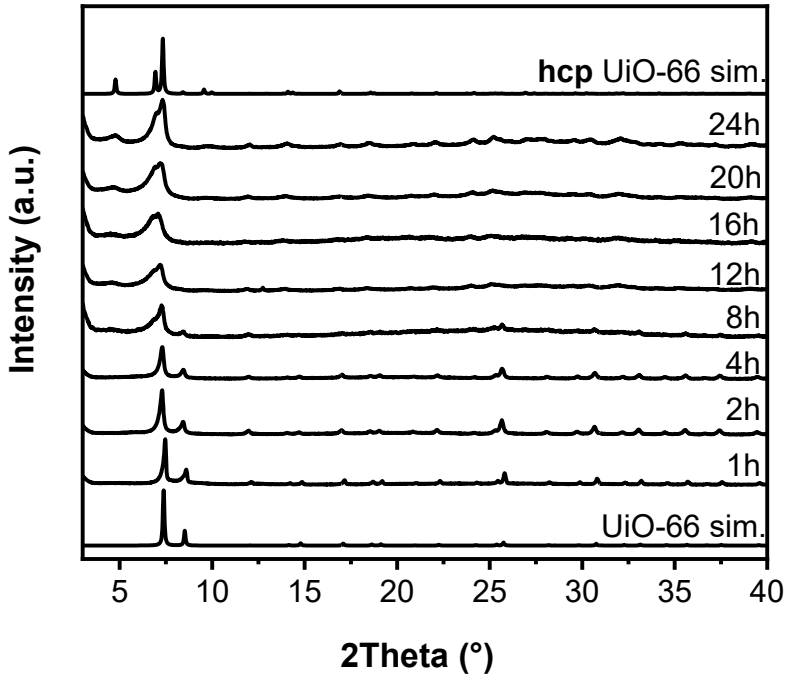


**Figure S15.** PXRD patterns of UiO-66-0.4 treated in aqueous solution of acetic acid (50%, v/v) at 150 °C with different durations.

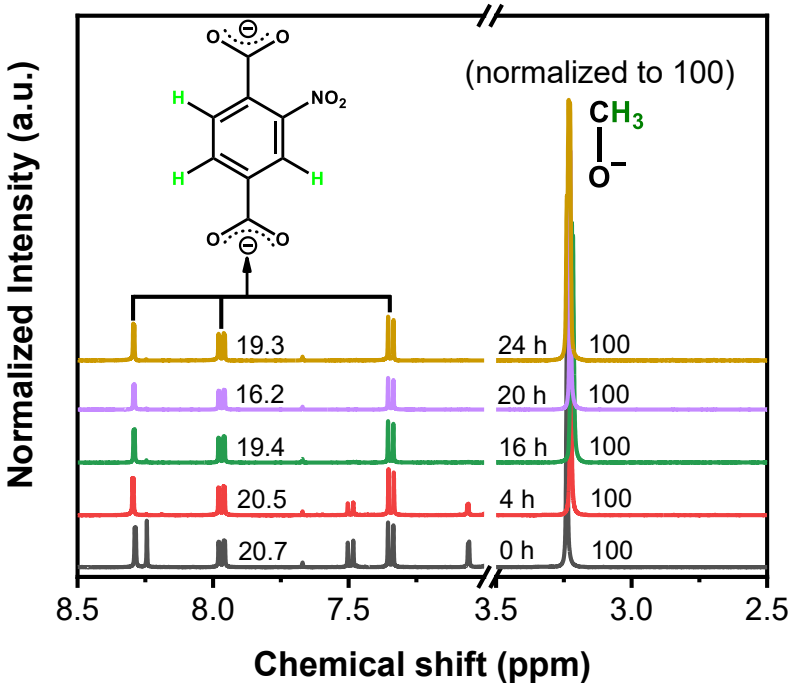


**Figure S16.** $^{1}$H NMR spectra of UiO-66-0.4 with various MICT durations. 10 mg solid sample was dissolved in 1 mL NaOH/$D_2O$ (1 M) and 20 μL methanol was added as the internal standard.

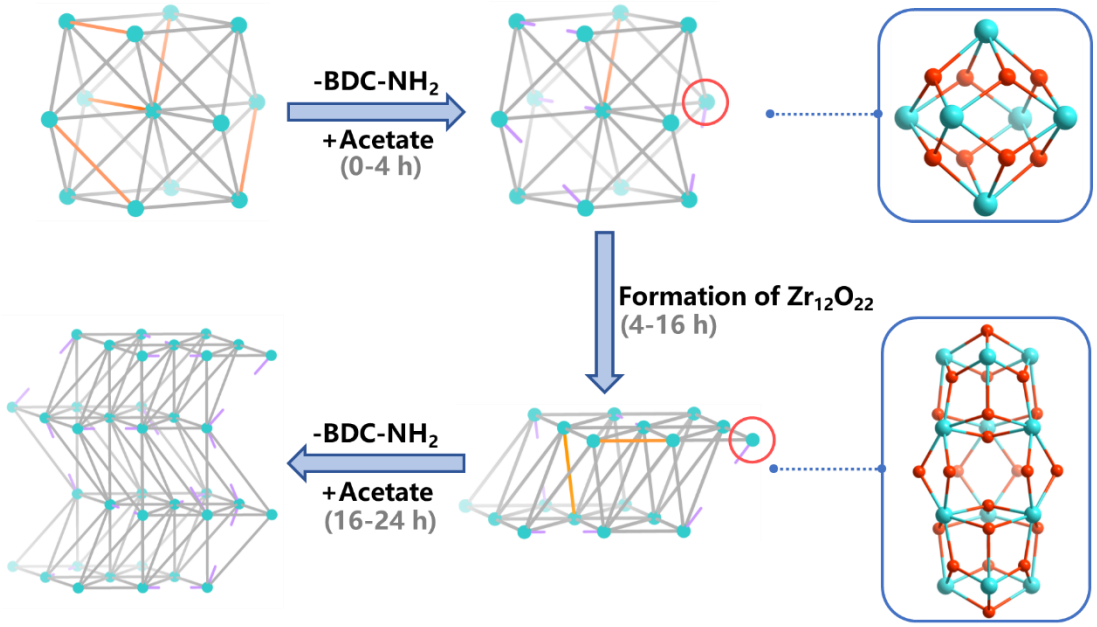


**Figure S17.** Proposed mechanism of the mixed-linker induced crystal transformation.

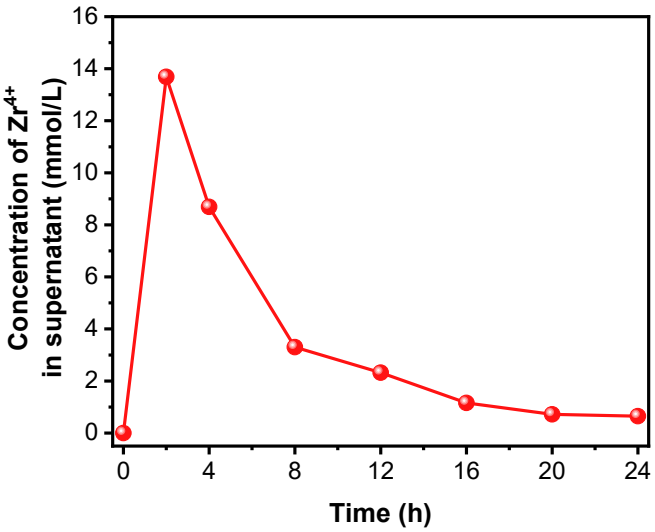


**Figure S18.** The concentration of $Zr^{4+}$ in synthetic supernatant with different reaction durations. (Synthetic conditions: UiO-66 150 mg, acetic acid 10 mL, $H_2O$ 10 mL, 150 ℃)

**Table S5.** Catalytic performance of the MOF samples in ring-opening reaction of styrene oxide with various alcohols.

| Epoxides | Alcohol | Catalyst | Conversion of Epoxides (%) |
|---|---|---|---|
| Styrene oxide | Methanol | blank | 5.7±0.7 |
| | | UiO-66 | 15.9±2 |
| | | UiO-66-$NO_2$ | 25.7±3.1 |
| | | **hcp** UiO-66 | 30.3±4.6 |
| | | **hcp** $NO_2$-FA | 28.8±2.3 |
| | | 0.2-AA | 75.1±4.6 |
| | | 0.4-AA | 83.5±4.2 |
| | | 0.6-AA | 89.0±5.8 |
| | Ethanol | blank | 0.8±0.1 |
| | | UiO-66 | 12.7±1.9 |
| | | UiO-66-$NO_2$ | 18.6±2.1 |
| | | **hcp** UiO-66 | 26.5±3.0 |
| | | **hcp** $NO_2$-FA | 23.3±1.7 |
| | | 0.2-AA | 67.7±4.9 |
| | | 0.4-AA | 76.4±3.6 |
| | | 0.6-AA | 84.2±4.4 |
| | Isopropanol | blank | 0.1±0.0 |
| | | UiO-66 | 9.1±0.3 |
| | | UiO-66-$NO_2$ | 7.9±0.9 |
| | | **hcp** UiO-66 | 16.8±1.5 |
| | | **hcp** $NO_2$-FA | 17.3±2.1 |
| | | 0.2-AA | 60.5±3.7 |
| | | 0.4-AA | 70.1±3.6 |
| | | 0.6-AA | 80.3±5.2 |
| | *tert*-Butyl alcohol | blank | 0.0±0.0 |
| | | UiO-66 | 2.2±0.3 |
| | | UiO-66-$NO_2$ | 1.3±0.2 |
| | | **hcp** UiO-66 | 7.9±1.9 |
| | | **hcp** $NO_2$-FA | 9.3±1.1 |
| | | 0.2-AA | 55.4±4.4 |
| | | 0.4-AA | 67.9±3.7 |
| | | 0.6-AA | 77.5±6.5 |

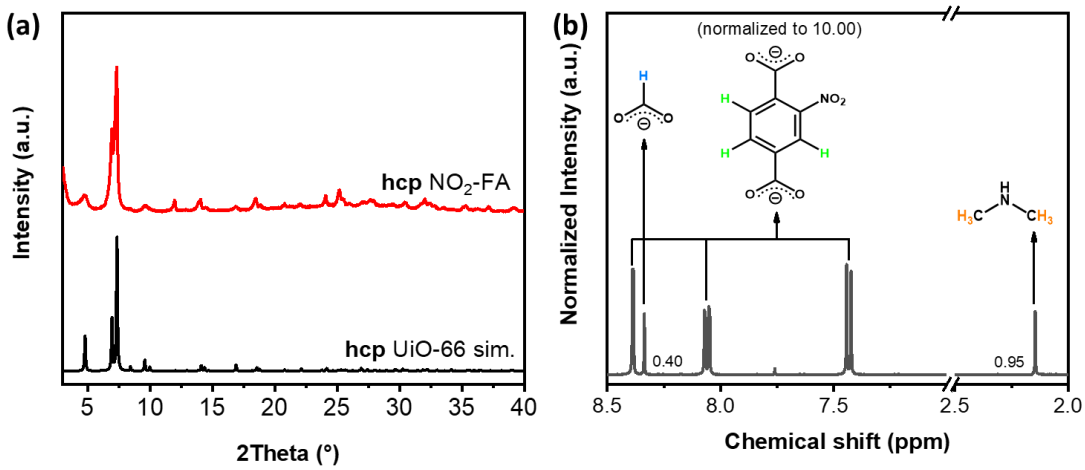


**Figure S19.** PXRD pattern (a) and $^{1}$H NMR spectra (b) of **hcp** $NO_2$-FA.

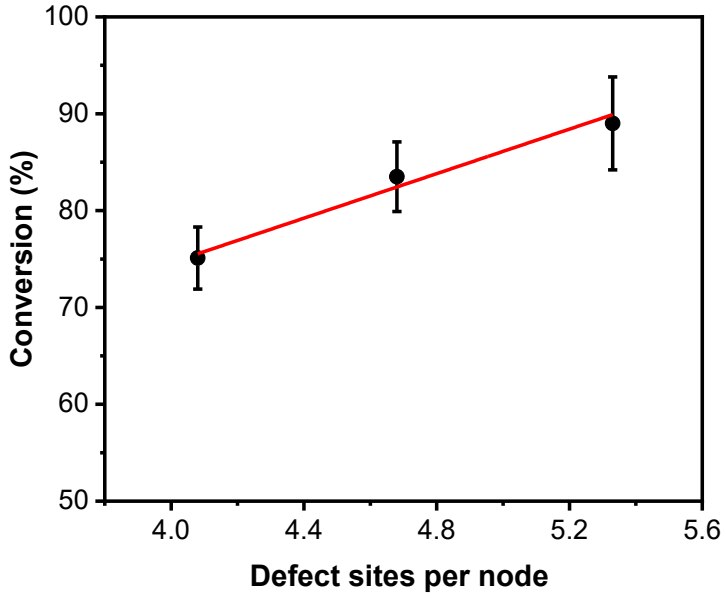


**Figure S20.** Correlation between styrene oxide conversion and the number of defect sites per node in **hcp** UiO-66-$NO_2$.

**Table S6.** statistical analysis of the catalytic data of 0.2-AA, 0.4-AA and 0.6-AA.

| MS | F | P-value | F crit |
|---|---|---|---|
| 147.75 | 76.32 | 0.00065 | 6.94 |

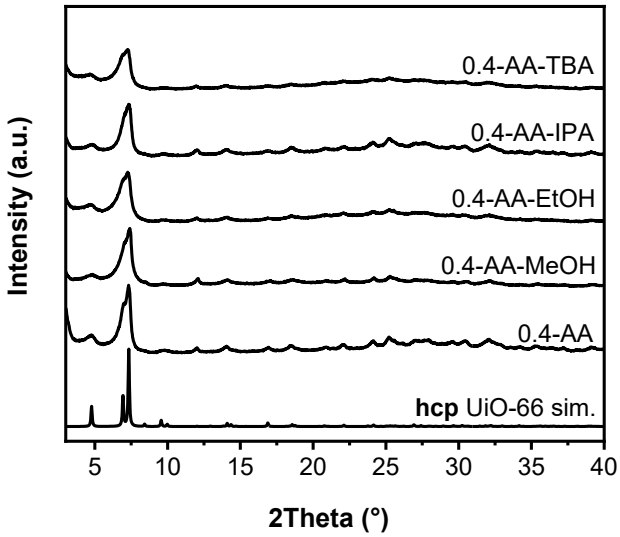


**Figure S21.** PXRD patterns of 0.4-AA before and after ring-opening reaction with various alcohols.

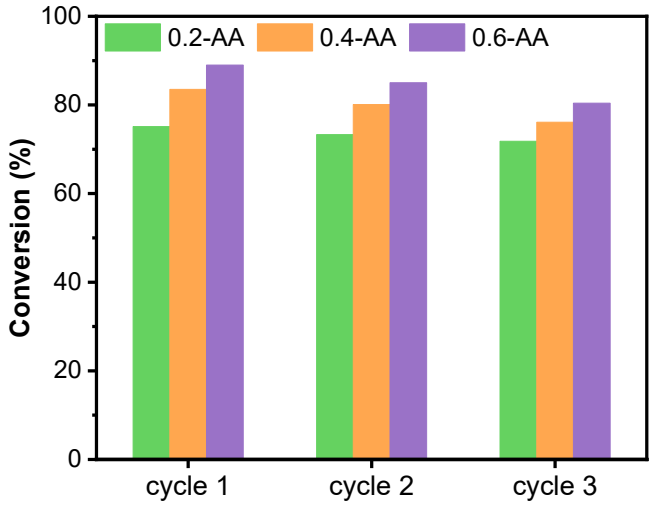


**Figure S22.** Reusability test of **hcp** UiO-66-$NO_2$ in ring-opening reaction of styrene oxide with methanol. The reused catalyst was wash with methanol for several times and activated at 120 ℃ for 12 h.

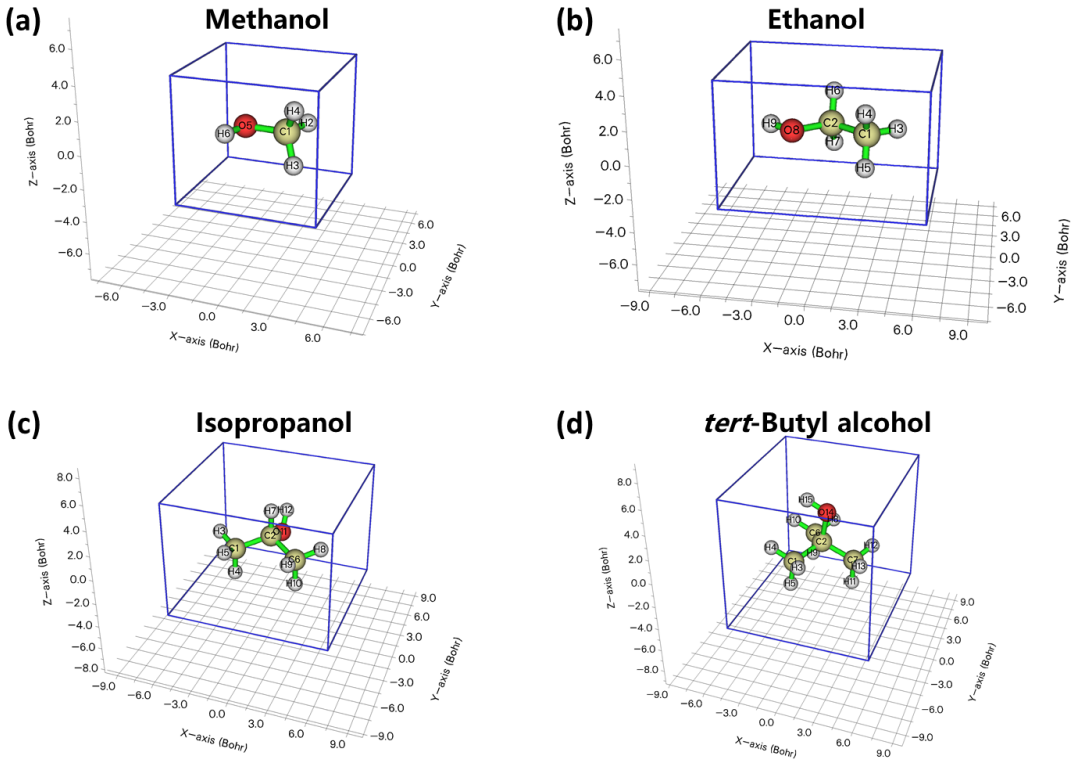


**Figure S23.** Molecular dimension of different reactant alcohols.

## Reference


1. Y. Xiao, L. Han, L. X. Zhang, B. C. Gates and D. Yang, *J. Phys. Chem. Lett.*, 2021, **12**, 6085-6089.
2. K. Tan, H. Pandey, H. Wang, E. Velasco, K.-Y. Wang, H.-C. Zhou, J. Li and T. Thonhauser, *J. Am. Chem. Soc.*, 2021, **143**, 6328-6332.